CSIRO PUBLISHING

International Journal of Wildland Fire **2014**, *23*, 733–745
http://dx.doi.org/10.1071/WF13159

The temporal evolution of wildfire ash and implications for post-fire infiltration

Victoria N. Balfour[A,D], *Stefan H. Doerr*[B] *and Peter R. Robichaud*[C]

[A]Department of Ecosystem and Conservation Sciences, University of Montana, 32 Campus Drive, Missoula, MT 59812, USA.
[B]Department of Geography, University of Wales Swansea, Singleton Park, Swansea, SA2 8PP, UK.
[C]US Department of Agriculture, Forest Service, Rocky Mountain Research Station, Forestry Science Laboratory, 1221 South Main Street, Moscow, ID 83843, USA.
[D]Corresponding author. Email: vnbalfour@gmail.com

Abstract. Changes in the properties of an ash layer with time may affect the amount of post-fire runoff, particularly by the formation of ash surface crusts. The formation of depositional crusts by ash have been observed at the pore and plot scales, but the causes and temporal evolution of ash layers and associated crusts have not yet been thoroughly investigated. In the long term, ash crusting effects will decrease as the ash layer is removed by wind and water erosion, but in the short term ash crusting could contribute to the observed changes in post-fire runoff. This research addresses these topics by studying the evolution over time of highly combusted ash layers from two high-severity wildfires that occurred in Montana in 2011. More specifically, this research was designed to assess the potential for ash crusts to form and thereby contribute to the observed decreases in infiltration after forest fires. Results indicate that high-combustion ash can evolve due to post-fire rainfall. Plots that exhibited a visible ash crust also displayed a significant decrease in effective porosity and hydraulic conductivity. These decreases in ash layer characteristics were attributed to raindrop compaction and ash hydration resulting in the formation of carbonate crystals, which decreased effective porosity and flow within the ash layer. During this same time period, inorganic carbon content more than doubled from 11 to 26% and bulk density significantly increased from 0.22 to 0.39 g cm^{-3} on crusted plots. Although raindrop impact increased the robustness of the ash crust, mineralogical transformations must occur to produce a hydrologically relevant ash crust. These results indicate that post-fire rainfall is an important control on the properties of the ash layer after burning and on crust formation. The observed temporal changes indicate that the timing of ash sampling can alter the predictions as to whether the ash layer is effecting post-fire infiltration and runoff. Despite the reduction in infiltration capacity, the formation of post-fire ash crusts could prove beneficial to post-fire hazard mitigation by stabilising the ash layer, and reducing aeolian mixing and erosion.

Additional keywords: ash crust formation, ash evolution, wildfires.

Received 18 September 2013, accepted 4 March 2014, published online 10 June 2014

Introduction

Within days to months after wildfire activity ash layers are often redistributed from the soil surface by wind, surface runoff or by being incorporated into the soil (Schmidt and Noack 2000; Novara *et al.* 2011; Santín *et al.* 2012; Pereira *et al.* 2013). As a result, the effect of ash on infiltration is often considered to be confined to the first few storms (Larsen *et al.* 2009). However, the effect of ash on infiltration during these early events can be considerable, and there are cases where ash continues to affect the runoff response for several months after a fire (Cerdà 1998), suggesting that the effect of ash layers varies spatially and temporally. Changes with time in ash layer properties, such as porosity, thickness, water repellency and hydraulic conductivity may affect infiltration response. Although the formation of an ash depositional seal on the soil surface has been shown to decrease infiltration response at both the pore and plot scale (Onda *et al.* 2008; Woods and Balfour 2008), less is understood regarding the formation or hydrological importance of ash crusts atop thicker ash layers. Natural ash crusts have been observed *in situ* following high-severity wildfires, but the mode of formation is not fully understood (Fig. 1). The ability of ash to form a crust was first suggested by Onda *et al.* (2008) where decreases in post-fire infiltration rates were attributed to the formation of a low-hydraulic-conductivity ash layer due to raindrop compaction. Gabet and Sternberg (2008) further noted that distinct ash layers reduced the ability of flowing water to infiltrate into underlying soil substrate during laboratory flume experiments, suggesting the possibility of an ash crust. During the same time Cerdà and Doerr (2008) suggested a mode of crust formation to be attributed to internal densification of the ash layer as it became compacted over time under its own weight. More recently, Balfour and Woods (2013) theorised that

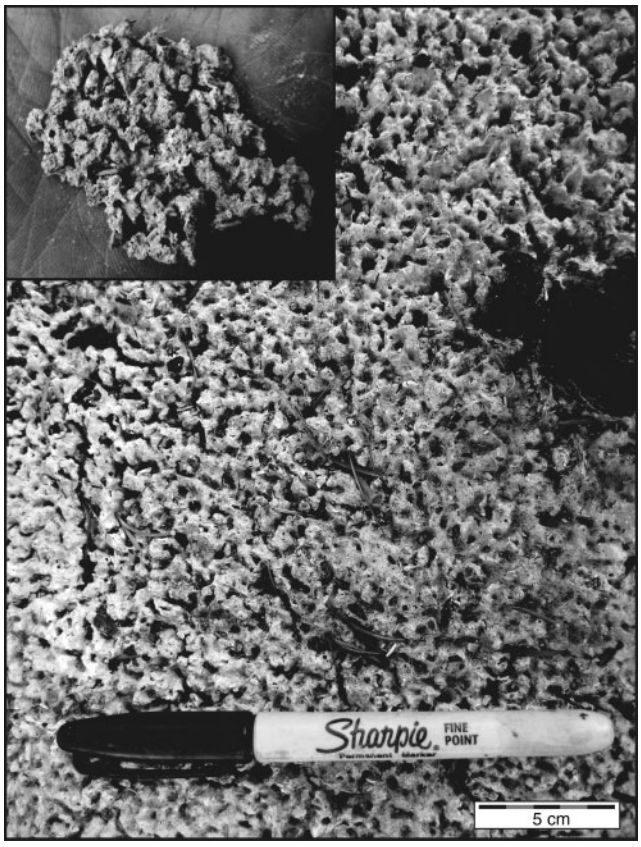

Fig. 1. A photograph of an ash crust at the 2009 Terrace Mountain wildfire, British Columbia, Canada (Balfour and Woods 2013). The inset photograph shows a 1.0 cm-thick piece of ash crust.

thermally produced oxides in highly combusted ash may be capable of forming a chemical crust, stabilising the ash layer and altering subsequent infiltration in post-fire systems. However, it is uncertain whether chemical crust formation by re-crystallisation within the ash layer can be caused simply by exposure of ash to air or whether direct rainfall is required to hydrate and compact the ash. Over the long term, the potential for ash crusts to form will undoubtedly decrease as the ash layer is removed via wind and water erosion, or is incorporated into the soil. However, changes in ash layer evolution as well as the formation of a surface ash crust may further explain variation in the hydrological response of ash in recently burnt ecosystems.

Understanding temporal changes in post-fire infiltration rates and the role of ash crust formation is essential for accurately modelling post-fire hydrologic processes (Robichaud 2000; Pierson *et al.* 2001). Although research regarding the effect of ash on infiltration and runoff is currently focussed on quantifying the hydrological properties of ash to facilitate the parameterisation of hydrologic models (Moody *et al.* 2009; Ebel *et al.* 2012), less attention is being applied to understanding if and how ash layers may evolve or change over time. To the authors current knowledge only one study has specifically documented spatio–temporal variation in ash layer thickness following a boreal grassland fire (Pereira *et al.* 2013). The lack of investigation into understanding ash evolution represents a significant research gap for the following reasons. First, there is a clear theoretical basis for ash layers to form crusts based on physical–chemical changes that have been documented to occur in vegetative ash combusted at high temperatures, either from wildfire or laboratory settings (Liodakis *et al.* 2005; Úbeda *et al.* 2009; Balfour and Woods 2013). Further, numerous authors have theorised that ash associated with high combustion temperatures, thus containing oxides and carbonates, could compact above the soil surface reducing ash hydraulic conductivity and promoting Hortonian overland flow (Cerdà and Doerr 2008; Onda *et al.* 2008; Woods and Balfour 2008). Preliminary tests conducted before this study indicated the formation of a chemically produced ash crust was possible following the hydration of wildfire ash containing oxides in the laboratory, suggesting a similar process may lead to the formation of chemical ash surface crusts in the field. Second, the lack of information regarding how ash layers change in the initial weeks after a fire limits the ability to develop refined models to predict fire-related flooding and erosion events. In order for post-fire models to be the most effective, they must accurately represent the infiltration, runoff and erosion processes taking place and therefore account for any significant changes in ash layers over time. For example, if ash crust formation alters infiltration in post-fire environments, then models need to account for this by incorporating ash-sealing effects into infiltration algorithms (Moody *et al.* 2009; Kinner and Moody 2010).

Research is still needed to systematically evaluate the effect of ash layer evolution on post-fire infiltration as well as to determine the conditions under which ash crusting occurs and its effect on subsequent infiltration response. The overall goal of this study was to address this research gap by examining changes in ash layer properties over time following high-severity wildfire activity in the Rocky Mountain region of the Western US. The specific aims were to (i) determine if the temporal evolution of *in situ* ash layers alters ash infiltration, (ii) document the formation of a post-wildfire ash crust, (iii) assess if ash crust formation was due to compaction by raindrop impact or mineralogical transformations associated with hydration and (iv) determine if mineralogical transformations associated with crust formation were dependent upon direct hydration or exposure to moist air.

Methods

Study sites and plot manipulation types

Study areas were located in two separate 2011 western Montana wildfires: the West Riverside wildfire (WR, 46°52′58.8″N, 113°53′16.8″W) and the Avalanche Butte wildfire (AV, 46°41′2.3994″N, 111°22′44.4″W). The WR wildfire started 22 August and consumed 1538 ha of mixed conifer forest (*Pinus contorta, P. ponderosa* and *Pseudotsuga menziesii*). The AV wildfire ignited 26 July and burnt 16 ha of subalpine fir (*Abies lasiocarpa*) and white bark pine (*P. albicaulis*). Based on the national incident information system (Inciweb, http://www.inciweb.org, accessed 12 June 2013) and field-based visual indicators (90–100% charred canopy, complete shrub and litter consumption, white and grey ash dominant) both

Table 1. Summary information for site characteristics of plots allocated to each type of plot manipulation in the West Riverside and Avalanche Butte wildfire study areas

Within and across plot manipulation types, variation in site characteristics were not significant ($P > 0.05$). Colour codes follow the Munsell (1975, p. 58) soil chart

					Ash			Soil	
Study area Treatment		Aspect (degrees)	Slope (%)	Depth (cm)	Ash clay/silt/sand (%)	Colour	Water repellency (s)	hydraulic conductivity (mm s^{-1})	Clay/silt/sand (%)
	n	6	6	60	18	18	30	18	18
West Riverside									
Natural	Mean	219	22	5.30	3/47/49	10YR 7/1	296	0.00328	6/66/20
	s.d.	21	3	0.83	2/5/5	–	94	0.00192	3/3/2
Screen	Mean	237	21	5.47	5/45/49	10YR 7/2	312	0.0024	6/68/20
	s.d.	19	3	0.72	2/4/4	–	70	0.00352	3/3/3
Cover	Mean	228	18	5.48	5/47/48	10YR 7/1	303	0.00439	7/71/20
	s.d.	26	2	0.59	2/3/3	–	98	0.00215	3/4/4
Overall	Mean	228	20	5.42	5/47/49	10YR 7/1	303	0.00373	7/68/25
	s.d.	22	3	0.72	2/4/4	–	87	0.00205	3/4/4
Avalanche Butte									
Natural	Mean	225	13	3.76	7/41/53	10YR 6/1	317	0.00379	7/60/33
	s.d.	18	2	1.13	3/7/6	–	72	0.00161	2/5/4
Screen	Mean	239	11	3.50	31/8/61	10YR 6/1	343	0.00386	6/65/29
	s.d.	12	3	1.12	3/8/7	–	48	0.00148	2/4/3
Cover	Mean	245	15	3.71	7/36/57	10YR 6/1	304	0.00411	4/66/30
	s.d.	7	2	1.24	2/9/8	–	125	0.0016	1/4/4
Overall	Mean	236	13	3.65	7/36/57	10YR 6/1	321	0.00392	6/64/31
	s.d.	14	2	1.16	3/9/8	–	88	0.00154	2/5/4

wildfires were classified as severe (Table 1; Neary *et al.* 2005; Parsons *et al.* 2010). The mean annual precipitation for the WR and AV areas were 350 and 290 mm (National Oceanic and Atmospheric Administration, http://www.nws.noaa.gov, accessed 28 June 2013).

In each study area, six sites were established that had similar ash colour and depth (Fig. 2). All sites were situated with a south-west aspect, and had slopes ranging from 16 to 27% in the WR area and 9 to 17% in the AV area (Table 1). A tipping bucket rain gauge and data logger were installed at each study site to monitor changes in precipitation. In order to determine the effect of raindrop impact and ash hydration on ash crust formation three 4-m^2 manipulation plots were installed at each site. At each site, one plot was exposed to natural rainfall, one was sheltered from rainfall by a canopy cover and the third was exposed to natural rainfall but protected from raindrop impact by a fine mesh screen. This design allowed one to distinguish the effects of natural rainfall on ash properties and ash crust formation as opposed to rainfall with minimal raindrop impact and the exposure of the ash layer to moist air but without direct hydration. The evolution of ash layer characteristics was measured at each plot over time in response to natural rainfall to gauge if *in situ* wildfire ash layers displayed similar alterations to wetting as documented in laboratory settings (Table 2; Stoof *et al.* 2010; Bodí *et al.* 2011, 2012; Bodí 2012; Balfour and Woods 2013) and were capable of producing an ash crust in the field.

Site characteristics and field measurements

Initial ash characteristics were recorded every 10 days for ~1 month. Sites were accessed as soon as possible according to safety standards. AV sites were assessed 11 days after complete containment whereas WR sites were assessed 6 days before complete containment. Field measurement sets were collected within a designated 0.25 × 2 m-wide transect area at plots at WR on 15 and 25 September as well as 2, 9 and 19 October and at AV on 14 and 23 August as well as 2, 8 and 28 September (Fig. 2). Ash field measurement sets (Table 1) consisted of water repellency ($n = 10$), colour ($n = 3$), infiltration ($n = 3$), thickness ($n = 10$) and bulk density ($n = 3$). Prior to each measurement set the percentage of ash, bare soil and rocks in the transect area were recorded using a 2 × 10-cm cell grid. The wettability of ash can vary from water repellent to rapidly wettable, thus altering the hydrological response (Bodí *et al.* 2011). Therefore the water drop penetration time test (DeBano *et al.* 1998) was used to measure ash wettability randomly in the transect area. Ash colour was recorded using the Munsell (1975, p. 58) soil colour chart. Ash infiltration was measured randomly in the transect area using a mini-disc tension infiltrometer (4.4-cm diameter, 2.0-cm tension, Decagon Devices 2006). This method was chosen because the mini-disc is already established for collecting qualitative measurements in post-fire settings (Robichaud *et al.* 2008; Moody *et al.* 2009). Ash layers, however, can be highly absorptive with reports of the entire capacity of the mini-disc (90 mL) infiltrating into the ash in less than 1 min (Moody *et al.* 2009; Balfour and Woods 2013). Therefore, before infiltration measurements were taken, a core ring (4.4-cm diameter) was inserted into the ash layer to limit lateral flow to one dimension. After infiltration readings were conducted, a trench was dug exposing the ash–soil interface as well as visually assessing for ash crusts. A 1.0-mm diameter pin was

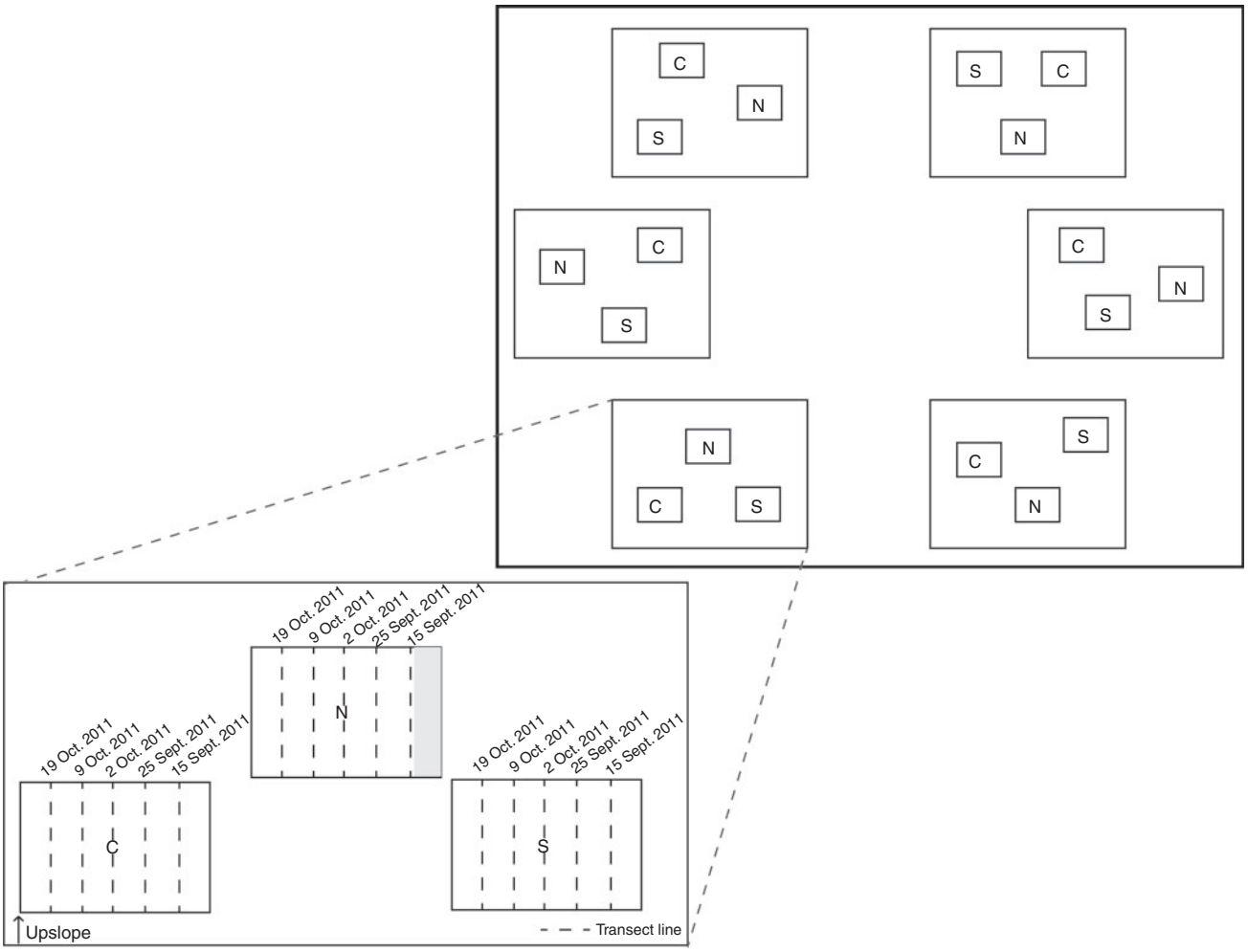

Fig. 2. A schematic layout depicting six sites designated within each wildfire study area. Each site contained three 2 × 2-m plots, which were randomly assigned a plot manipulation type; cover (C), natural (N) or screen (S). At each plot, data were collected from a 0.25 × 2-m transect area (represented in grey) for each allocated collection date. Dates shown in this figure correspond to West Riverside site collection.

Table 2. Ash characteristics measured and established methodology

Ash characteristic	Method	Location	Citation
Colour	Soil colour chart	Field	Munsell (1975, p. 58)
Particle size distribution	Laser diffractometer	Laboratory	Balfour and Woods (2013)
Bulk density	Soil core	Field	Grossman and Reinsch (2002)
Inorganic, organic carbon	CNS analyser	Laboratory	Schumacher (2002)
Mineralogy	X-Ray diffraction	Laboratory	Etiégni and Campbell (1991); Balfour and Woods (2013)
Effective porosity	Gravimeteric saturation	Field	Flint and Flint (2002)
Sorptivity	Mini-disc tension Infiltrometer	Field	Vandervaere *et al.* (2000); Clothier and Scotter (2002); Moody *et al.* (2009)
Water repellency	Water drop penetration time	Field	Bodí *et al.* (2011)
Hydraulic conductivity	Mini-disc tension Infiltrometer	Field	Moody *et al.* (2009); Ebel *et al.* (2012); Balfour and Woods (2013)

then inserted at 10 locations along the trench to compute a mean ash thickness. To avoid soil contamination the full thickness of the ash layer was not sampled during bulk density collection; instead a soil core was used to sample the ash layer to a depth ~0.5 cm above the ash–soil interface. All field-based measurements were taken in triplicate unless otherwise stated, and a composite ash sample was collected for laboratory analysis.

Following ash measurements, three random soil samples were collected at each plot to confirm consistent underlying soil texture conditions. Soil water repellency, with depth, was recorded in the transect area according to DeBano *et al.* (1998). The hydraulic conductivity of non-water repellent soil layers was measured in triplicate using a mini-disc tension infiltrometer.

Calculations and laboratory analysis

Laboratory analysis consisted of ash mineralogy, effective porosity, particle size distribution, and organic and inorganic carbon content (Table 1). X-Ray diffraction analysis was used to identify ash mineralogy and changes in ash composition associated with hydration over time (Etiégni and Campbell 1991; Balfour and Woods 2013). Existing values of ash porosity are typically based on total porosity, but internal ash pores (Balfour and Woods 2013) may alter porosity readings so effective porosity was determined via the gravimetric saturation method (Flint and Flint 2002). Organic and inorganic carbon contents were determined via a dry combustion CNS analyser (Model EA1100, Fisons Instruments, Milan, Italy) and CO_2 emissions in accordance with Schumacher (2002). Soil and ash particle size distribution were determined using laser diffractometry after sieving samples to less than 2.0 mm (Malvern Instruments Ltd, Malvern, UK; Balfour and Woods 2013), with the percentage of the sample greater than 2.0 mm recorded as coarse fragments.

Values for ash and soil hydraulic conductivity (K, mm s^{-1}) were computed using a second-order polynomial function to fit cumulative infiltration to the square root of time (Dane and Hopmans 2002; Decagon Devices 2006), an established method for ash hydraulic conductivity (Moody *et al.* 2009; Ebel *et al.* 2012; Balfour and Woods 2013).

Values for ash sorptivity (S, mm $s^{-0.5}$) were computed as the slope of the linear regression cumulative infiltration *v.* the square-root of time (Vandervaere *et al.* 2000; Clothier and Scotter 2002; Moody *et al.* 2009).

Statistical analysis

Between-wildfire variability was not compared as the study only aimed at addressing within-wildfire variability of ash characteristics over time. One-way ANOVAs were conducted on initial site and plot characteristics (aspect, slope, ash depth, soil hydraulic conductivity and water repellency) to assess variation across sites and plots for each wildfire. Repeated one-way ANOVAs were conducted on the following variables to assess variation in ash characteristics over time at plots of similar manipulation type: depth, bulk density, effective porosity, water repellency, sorptivity, hydraulic conductivity, ground cover, and organic and inorganic carbon content. One-way ANOVAs were also used to test for differences between manipulation types (natural, screen, cover) for each measurement date. Prior to ANOVAs, the variables were tested for normality using the Kolmogorov–Smirnov test. Statistical analysis was conducted using SPSS software (SPSS for Windows, ver. 10.0.5 (27 November 1999), SPSS Inc., Chicago, IL). Only $P < 0.05$ are reported as significant in the results.

Results

Site characteristics and rainfall

Prior to initial data collection, ash layers at all plots were dry to the touch with no evidence of rainfall or compaction. Within and across plot manipulation types, variation in site and plot characteristics was not significant. All plots were 100% covered with grey (10YR 6/1) to light grey (10YR 7/1) ash with overall mean thicknesses of 54 ± 7 mm and 37 ± 11 mm for WR and AV plots. All ash layers were hydrophilic (water drop penetration time (WDPT) < 0.5 s) and the initial characteristics (depth, bulk density, carbon content and colour) were consistent within and across plot manipulation types (Table 3). Initial ash hydraulic conductivity and sorptivity values were consistent across plots at each wildfire site, with rates of 0.107 ± 0.0034 mm s^{-1} and 1.47 ± 0.33 mm $s^{-0.5}$ for WR plots and 0.032 ± 0.0062 mm s^{-1} and 1.15 ± 0.46 mm $s^{-0.5}$ for AV plots (Fig. 3).

The underlying soil texture of all plots, irrespective of site location, was a gravelly silt loam (Table 1). Underlying soils were highly water repellent with the overall mean WDPT > 300 s. Underlying soil contained a mean hydraulic conductivity of 0.00373 ± 0.00021 mm s^{-1} and 0.00392 ± 0.0015 mm s^{-1} in WR and AV (Table 1). Soil water repellency and hydraulic conductivity were not variable across plots at each site or between sites for each wildfire (Table 1).

In WR and AV areas, precipitation did not significantly vary across sites and two storm events were recorded during data collection. The first storm at WR occurred on 22 September 2011 as a brief low-intensity (10 mm h^{-1}) event lasting 30 min. A natural plot, which was situated approximately 1 m downslope from a patch of bare, water repellent soil, was exposed to overland flow following this event. Visual assessment indicated that the ash layer absorbed the flow and an ash crust had formed by the time of reassessment 3 days later (Fig. 4). The second rainfall event was much larger and occurred on 17 October 2011, producing 20 mm of rain over a 30-min period. This storm resulted in substantial overland flow into adjacent unburnt areas, the formation of inter-rills in the ash crust, and erosion and substantial removal of large portions of the ash layer (Fig. 5). The first storm event to occur at AV was of low intensity (8 mm h^{-1}) and duration (15 min) on 20 August 2011, with no signs of overland flow or erosion. The second rainfall event occurred on 15 September 2011 and produced 25 mm of rain over a 60-min period, resulting in erosion and the removal of large portions of the ash layer.

Temporal and plot manipulation variation

West Riverside (WR) wildfire

Ash crust formation was visually documented in screen and natural plots for the WR fire on 25 September. Between 15 and 25 September, inorganic carbon content more than doubled ($P < 0.01$) and bulk density significantly increased from 0.22 to 0.39 g cm^{-3} ($P < 0.05$) for natural and screen plots (Table 3). Associated with these alterations was a darkening of the dry ash colour (not observed in cover plots), as well as a loss of relative oxides present in the ash and an increase in carbonate on 25 September. Mineral identification from X-ray diffraction (XRD) analysis indicated oxides only present in samples collected on 15 September. It should be noted that oxides in XRD

Table 3. Summary information for plot characteristics of ash exposed to varying types of plot manipulation (natural, cover and screen) at the West Riverside and Avalanche Butte study areas over the allotted collection periods

Probabilities over time for similar plot manipulation types are significant at: *, $P < 0.05$; **, $P < 0.01$. Colour codes follow the Munsell (1975, p. 58) soil chart

		Natural					Screen					Cover				
Study area Date		Depth (cm)	Bulk density (g cm^{-3})	Organic C (%)	Inorganic C (%)	Colour	Depth (cm)	Bulk density (g cm^{-3})	Organic C (%)	Inorganic C (%)	Colour	Depth (cm)	Bulk density (g cm^{-3})	Organic C (%)	Inorganic C (%)	Colour
	n	60	18	6	6	18	60	18	6	6	18	60	18	6	6	18
West Riverside																
15 Sept.	Mean	5.30	0.22	4.70	11.87	10YR 7/1	5.47	0.22	5.35	10.44	10YR 7/2	5.48	0.23	5.59	10.96	10YR 7/1
	s.d.	0.83	0.04	3.83	3.88	–	0.72	0.03	3.68	2.78	–	0.59	0.04	2.62	3.58	–
25 Sept.	Mean	3.9*	0.39*	8.09	26.95**	10YR 5/1	3.91*	0.38*	7.60	23.01**	10YR 6/1	3.94*	0.23	6.32	10.06	10YR 7/1
	s.d.	0.70	0.04	2.87	6.95	–	0.70	0.05	3.01	10.18	–	0.80	0.03	3.38	2.80	–
2 Oct.	Mean	3.83	0.40	6.68	29.62	10YR 5/1	3.76	0.38	6.83	22.03	10YR 6/1	2.85*	0.24	6.71	11.25	10YR 7/1
	s.d.	0.64	0.05	4.60	9.05	–	0.66	0.05	3.88	10.18	–	0.92	0.04	3.42	4.32	–
9 Oct.	Mean	3.86	0.40	8.01	26.69	10YR 3/1	1.95*	0.38	6.08	22.03	10YR 5/1	1.56*	0.23	7.12	11.28	10YR 5/1
	s.d.	0.69	0.03	3.58	8.89	–	0.57	0.04	3.61	11.52	–	0.85	0.04	3.08	3.57	–
19 Oct.	Mean	0.58*	0.43	6.15	32.74	10YR 3/1	0.56*	0.40	7.35	24.63	10YR 5/1	0.7*	0.25	6.65	9.48	10YR 5/1
	s.d.	0.25	0.06	3.42	7.89	–	0.23	0.05	2.71	10.66	–	0.31	0.04	2.94	3.27	–
Avalanche Butte																
14 Aug.	Mean	3.76	0.35	11.29	30.04	10YR 6/1	3.50	0.30	10.31	31.01	10YR 6/1	3.71	0.31	11.74	30.57	10YR 6/1
	s.d.	1.13	0.07	4.35	7.91	–	1.12	0.09	3.23	9.82	–	1.24	0.09	3.01	11.44	–
23 Aug.	Mean	2.28	0.36	10.19	27.56	10YR 4/1	2.26	0.35	9.99	27.12	10YR 4/1	1.99	0.29	13.06	26.51	10YR 4/1
	s.d.	0.84	0.05	3.81	7.28	–	0.87	0.06	3.18	8.44	–	0.65	0.06	3.29	12.81	–
2 Sept.	Mean	1.37	0.39	9.24	31.89	10YR 4/1	1.36	0.35	11.01	29.20	10YR 4/1	0.97	0.33	12.51	22.01	10YR 4/1
	s.d.	0.7	0.06	2.30	7.93	–	0.72	0.09	4.34	12.34	–	0.53	0.09	3.33	12.45	–
8 Sept.	Mean	1.63	0.36	11.33	32.20	10YR 4/1	1.57	0.33	10.56	28.62	10YR 4/1	1.53	0.30	11.15	25.09	10YR 4/1
	s.d.	0.44	0.06	3.67	7.92	–	0.44	0.09	4.66	8.70	–	0.40	0.10	3.01	6.88	–
28 Sept.	Mean	1.24	0.38	9.50	31.68	10YR 4/1	1.21	0.36	12.11	32.96	10YR 4/1	1.08	0.31	12.01	23.52	10YR 4/1
	s.d.	0.5	0.07	1.81	8.16	–	0.55	0.07	3.42	8.34	–	0.59	0.09	3.09	10.76	–

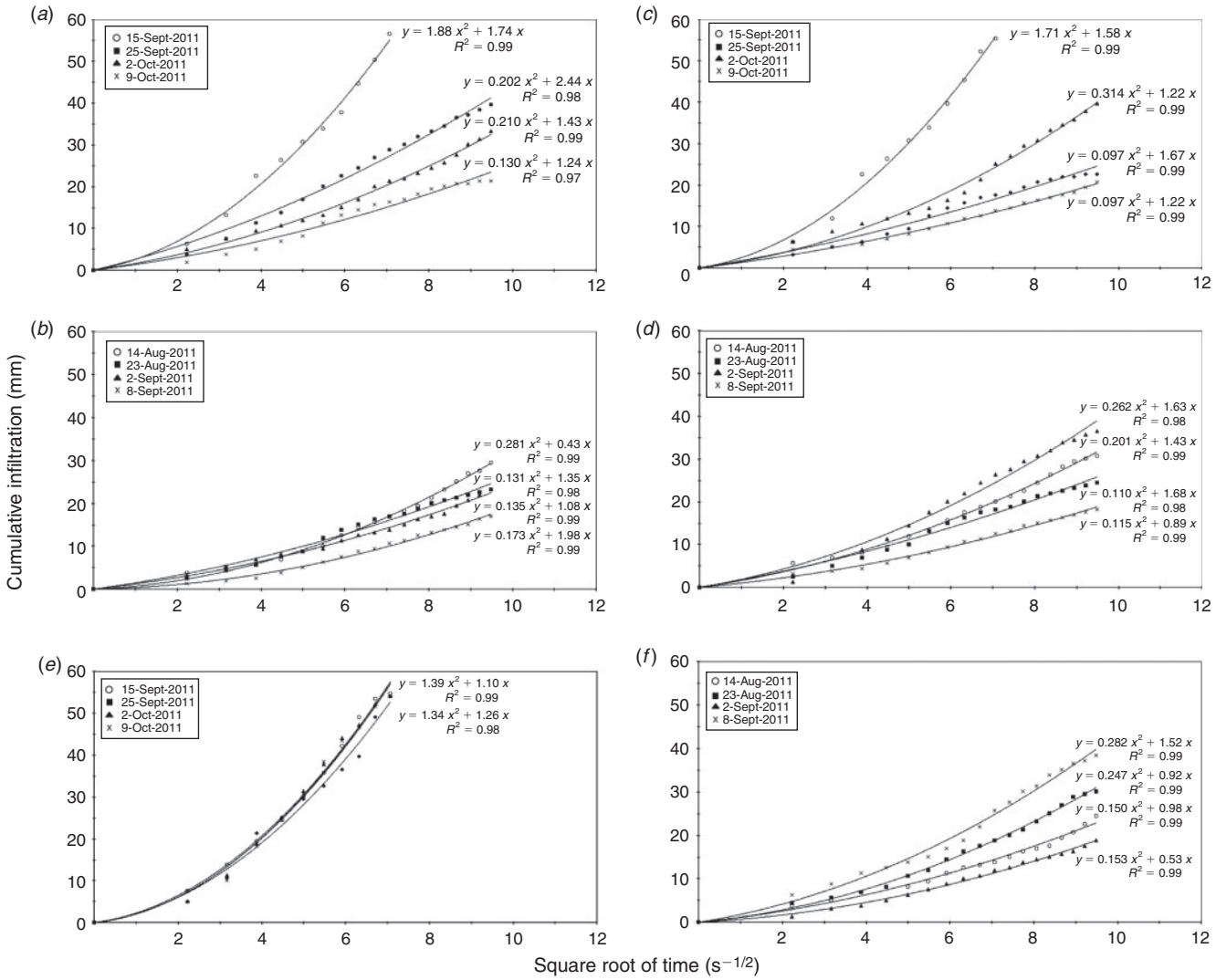

Fig. 3. Representative plots of ash infiltration measurements for the three different types of plot manipulation, natural (*a*, *b*), screen (*c*, *d*) and cover (*e*, *f*), in the West Riverside (top) and Avalanche Butte (bottom) wildfires over the allotted collection period. Infiltration data were not recorded on 19 October or 28 September for the West Riverside and Avalanche Butte sites, because of insufficient ash cover. The coefficient of the x^2 term is used to calculate hydraulic conductivity (mm s^{-1}) (Moody *et al.* 2009; Balfour 2014). The coefficient of the *x*-term is the sorptivity value (mm $s^{-0.5}$).

signatures were low and not present in all samples, but the increase in the relative intensities of carbonate on 25 September indicated a mineralogical shift. The initial (15 September) effective porosity was high for all plots, with values of 86 ± 3, 86 ± 2 and $87 \pm 3\%$ for natural, cover and screen. On 25 September a significant decrease in porosity was documented at natural and screen plots ($P < 0.01$; Fig. 6). Further decreases in porosity over time were not recorded in natural and screen plots. Covered plots did not exhibit significant changes in effective porosity over the course of the study.

Ash ground cover began to decrease on 25 September with screen and natural plots exhibiting 100% ash cover until 9 October (Fig. 7*a*). Bare soil significantly increased for all plots following the second rainfall event (17 October), resulting in ~50% bare soil (Fig. 7*a*). Regardless of plot manipulation type, variation in organic carbon content over time and across plot manipulation type were not significantly different. Ash depth at screen and natural plots significantly ($P < 0.05$) decreased for data collection on 25 September and again on 19 October, whereas depth at cover plots decreased continuously for all collection dates (Table 3). The mean initial hydraulic conductivity was 0.23 ± 0.14, 0.17 ± 0.06 and 0.21 ± 0.07 mm s^{-1} for natural, cover and screen (Fig. 3). Following the first rainfall event hydraulic conductivity at natural and screen plots decreased 1 order of magnitude, from 10^{-1} to 10^{-2} mm s^{-1} ($P < 0.01$), whereas cover plots indicated no significant change. All initial sorptivity values were within the range of 1.04–1.74 mm $s^{-0.5}$ and, regardless of plot manipulation type, there was no significant change over time (Fig. 3).

Avalanche Butte (AV) wildfire

Ash crust formation was not documented at any plots situated in the AV wildfire and no significant plot manipulation effect was noted at AV sites (Table 3). Initial inorganic carbon content

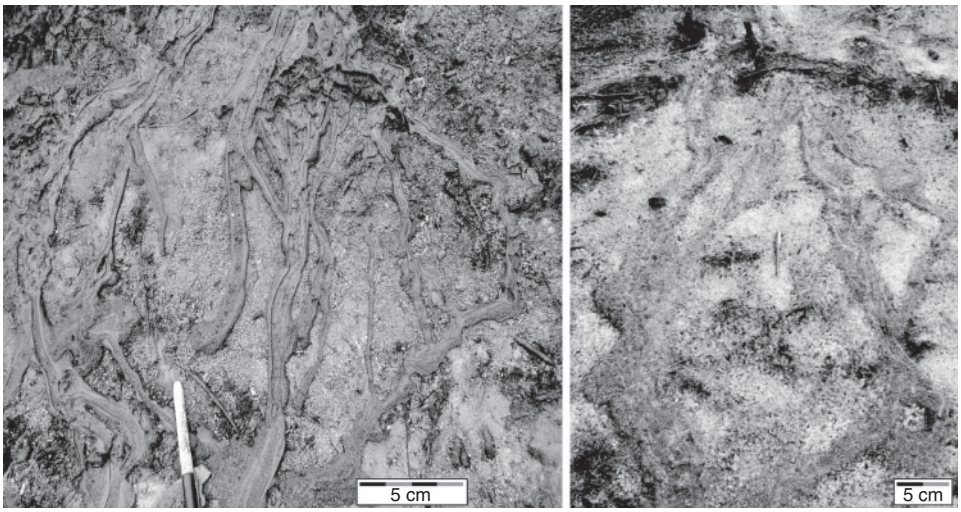

Fig. 4. Photographs of overland flow from adjacent hydrophobic soil onto an ash layer. Photographs were taken during the rainfall event (left) and 3 days after (right).

Fig. 5. Representative photographs of ash crust inter-rilling at natural and screen plots (left) as well as overland flow and erosion into adjacent unburnt areas (right).

(30%) was triple that of WR ash and did not change significantly over time (Table 3). X-Ray diffraction peaks were associated with silica and carbonate and no significant change occurred over time. Ash organic carbon content was low, ranging from 5 to 18% (Table 3). There was no significant change in ash organic content over time at any plot. Regardless of plot manipulation type or temporal variation, mean ash bulk density values were consistently within 0.05 of 0.34 g cm^{-3} for all plots (Table 3). Ash depth linearly decreased with time, but changes between subsequent dates were not significant. Ash ground cover began to decrease in all plots starting 23 August, with bare soil >50% on 28 September ($P < 0.05$; Fig. 7*b*). The mean initial ash hydraulic conductivity at all AV plots was 0.0323 ± 0.0058 mm s^{-1} (Fig. 3). Although ash hydraulic conductivity decreased over time, changes between subsequent dates were not significant and were less than 1 order of magnitude. Initial ash sorptivity values ranged from 0.43 to 2.01 mm s$^{-0.5}$ with no significant change over time, irrespective of plot manipulation type (Fig. 3). Initial effective porosity ranged from 69 to 88% and no significant change was documented over time, irrespective of plot manipulation type.

Discussion

Temporal changes in ash layer characteristics

The two wildfire sites in this study displayed contrasting results regarding changes in ash layer characteristics over time. The formation of an ash crust and subsequent changes in ash layer

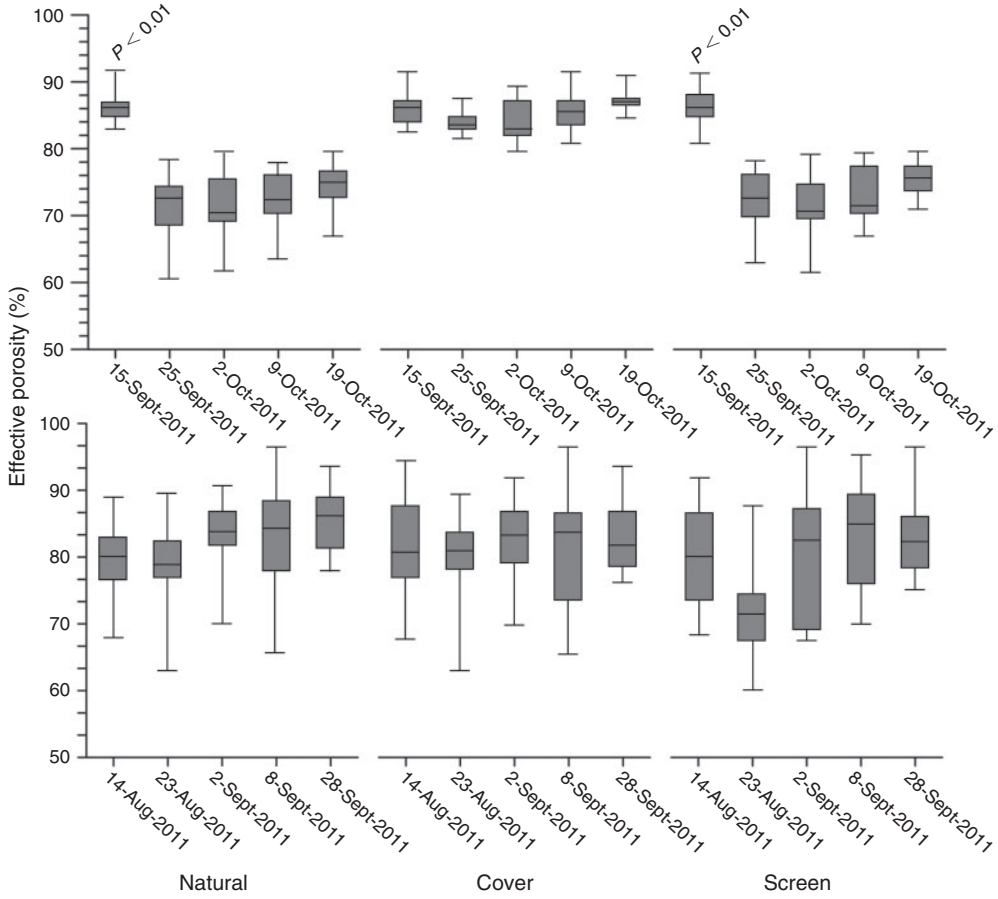

Fig. 6. Boxplots of effective porosity values for West Riverside (upper) and Avalanche Butte sites (lower). Significant differences are indicated with a *P*-value above the boxplot.

characteristics (decreases in porosity, bulk density and hydraulic conductivity) were documented to occur in WR ash layers, whereas ash in the AV wildfire did not show signs of ash crust formation or variation in ash layer characteristics over time. The most likely explanation for the contrasting effects is variation in initial ash chemical composition. Although both wildfires were classified as high severity and contained light grey (10YR 7/1) to grey (10YR 6/1) ash, WR sites contained ash with initially lower levels of carbonate and the presence of oxide (Table 3). This difference in the initial composition of the ash, which may be due to variation in fuel and burning conditions, suggests that chemical transformation and the production of hydrated carbonate are important components in the formation of an ash crust (Balfour and Woods 2013; Bodí *et al.* 2014).

To the authors' knowledge only one study has aimed at documenting changes in ash layer characteristics or evolution immediately after wildfire activity (Pereira *et al.* 2013). This paucity of research may be because of the fact that post-fire ash is often viewed as ephemeral: highly movable and often removed within days to months after a fire (Wagenbrenner *et al.* 2011). Data collected from the WR sites indicated variation in ash thickness and bare soil percentage was associated with the type of plot manipulation, as ash layers protected from hydration decreased in thickness and the percentage of bare soil increased continuously over time. However, ash thickness at 'natural' and 'screen' plots stabilised after the rain event on 25 September (Table 3, Fig. 7*a*). A study conducted at the hill-slope scale by Pereira *et al.* (2013) tracked the evolution of ash thickness over a 45-day period and attributed changes in thickness to redistribution by wind. Although wind erosion and wind speed were not assessed during the current study, the data suggest that continuing changes at 'cover' sites were due to redistribution by wind, whereas ash plots containing an ash crust were not as susceptible to wind redistribution and therefore more stable over time. This stability was indicated by a constant ash depth measured for 2 and 9 October at 'natural' WR and 2 October for 'screen' plots, in contrast to the constant decline in ash thickness at the un-crusted 'cover' plots. All plots at the AV sites displayed similar trends to un-crusted plots at WR sites (Table 3, Fig. 7*b*), again suggesting the absence of an ash crust may enhance aeolian erosion, as ash depth continuously decreased.

Sites that exhibited a visible ash crust (WR: natural and screen) also displayed a significant decrease in effective porosity ($P < 0.01$; Fig. 6), bulk density ($P < 0.05$; Table 3) and hydraulic conductivity ($P < 0.01$; Fig. 3). Whereas decreases in ash layer thickness over time can be associated with wind and water erosion (Bodí *et al.* 2014), the decreases in ash layer characteristics observed here were attributed to raindrop

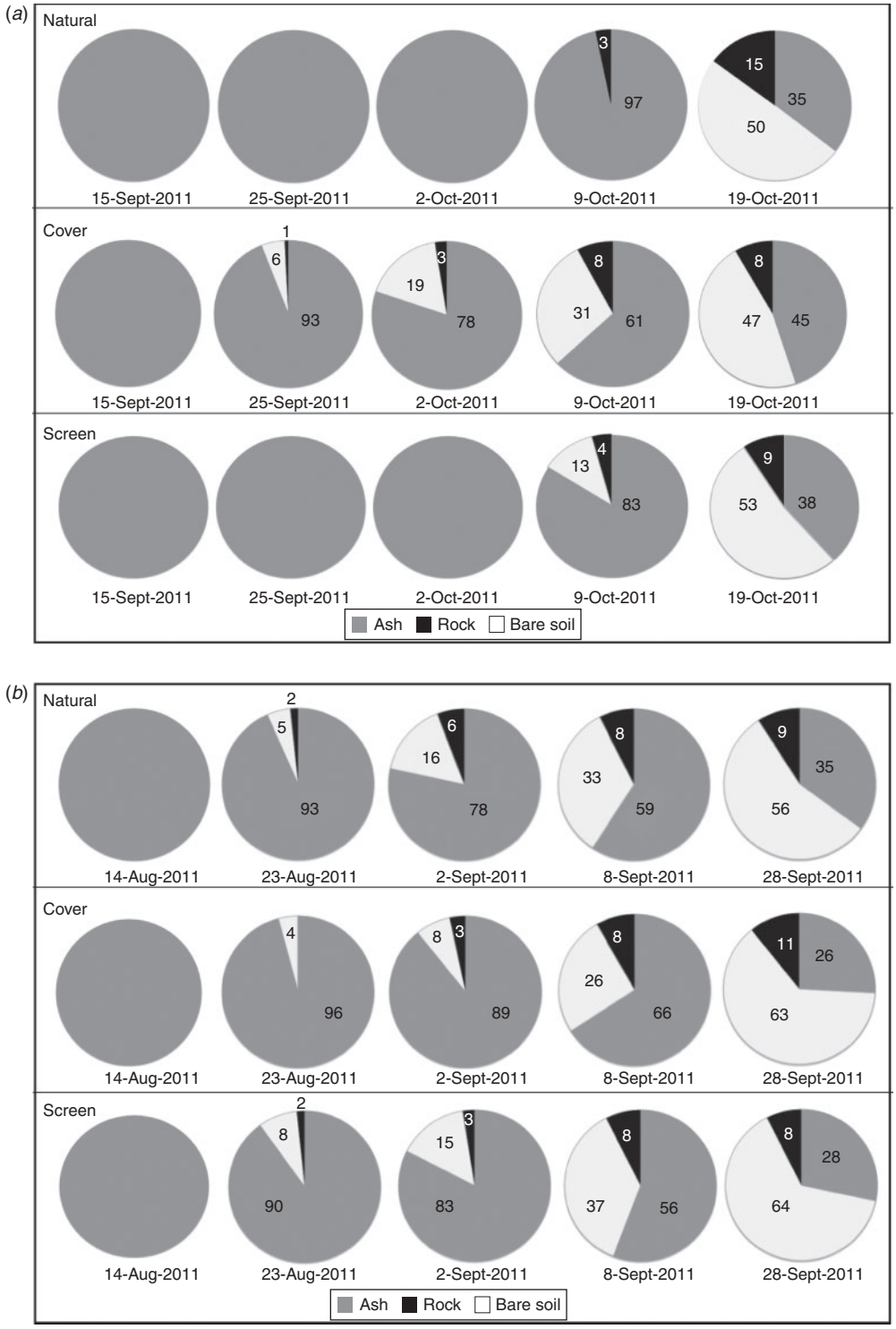

Fig. 7. Pie charts displaying the mean percentages of plot coverage for the three different types of plot manipulation (natural, cover and screen) in the (*a*) West Riverside and (*b*) Avalanche Butte wildfires over the collection period.

compaction and ash hydration resulting in the formation of carbonate crystals, which decreased effective porosity and flow within the ash layer (Balfour and Woods 2013). The conversion of oxides to carbonates has also been shown to decrease the packing density of ash by changing ash particle density (Balfour and Woods 2013). The formation of carbonate associated with crusting was confirmed by a doubling of inorganic carbon content at 'natural' and 'screen' plots following the 22 September rain event as well as a loss of oxide (Table 3). Woods and Balfour (2010) suggested that compaction of ash by raindrop

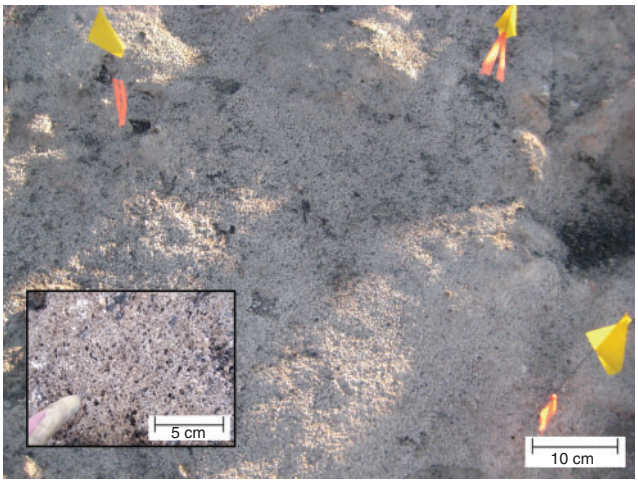

Fig. 8. Ash crust formed at the West Riverside site natural plots, after the initial rainfall event.

impact during initial post-fire rainfall may reduce the hydraulic conductivity of the ash layer. However, the current study found no difference between the hydrological response of plots with and without a screen, arguing against such a proposal. Results from this study do suggest that raindrop impact contributed to ash crust formation, subsequently reducing ash hydraulic conductivity (Fig. 3). Visual assessment of the ash crusts indicated cratering within the ash as a result of raindrop impact (Fig. 8). Temporal decreases in ash thickness suggest that raindrop impact also contributed to the formation of ash crusts. Results indicate that crusts formed under 'screen' plot manipulation began to erode before the large rainfall event (17 October), as ash thickness began to significantly ($P < 0.05$) decrease on 9 October (Table 3, Fig. 7*a*), suggesting crusts formed under 'screen' plot manipulations were not as stable as those formed under 'natural' conditions.

Mechanisms and significance of ash crust formation

Natural ash crusts have been observed *in situ* following high-severity wildfires (Onda *et al.* 2008; Woods and Balfour 2008; Balfour and Woods 2013; Bodí *et al.* 2014), but the mode of ash crust formation – whether internal densification (Cerdà and Doerr 2008), raindrop-induced compaction (Onda *et al.* 2008) or mineralogical transformations due to wetting (Balfour and Woods 2013) – has yet to be directly assessed. The initial light rainfall event that occurred at the WR wildfire in the current study hydrated the ash layer, which formed a crust via chemical transformations and raindrop impact. The data also indicate that raindrop impact alone was not sufficient to produce an ash crust, as only sites containing oxides, and initially low inorganic and organic carbon levels (Table 3), were observed to crust when exposed to direct hydration. Further, crust formation was observed in 'natural' and 'screen' plots, indicating that a chemical transformation, not raindrop impact, was the main mechanism of crust formation at 'screen' plots. The resultant hardened ash reported in this current study was associated with a substantially lower hydraulic conductivity, porosity and higher bulk density than unhardened ash (Figs 3, 6, Table 3).

Similar responses to those recorded in this study have been noted for other ecosystems of post-fire research. In Spain, Cerdà (1998) commented that the initial ash layer was highly absorptive, and the high infiltration rates were attributed to the low moisture content and high porosity of the ash layer. Four months later, however, infiltration decreased by more than 50%, with the ash layer reported to have 'crusted' on the soil surface. Following the 1995 Mount Vision Fire in California, raindrop impact significantly compacted the ash, increasing the runoff response by a factor of four relative to the first post-fire storm (Onda *et al.* 2008). A similar response was also noted for the laboratory setting by Gabet and Sternberg (2008), where the addition of a 1.0-cm ash layer increased runoff three to four times. Gabet and Sternberg attributed the increase to the ash layer decreasing infiltration to the underlying soil surface. However, it should be noted that the effects noted by Gabet and Sternberg (2008) are not the result of an ash crust but of sealing of the soil surface by ash particles, similar to the observations by Woods and Balfour (2010) of calcium-rich ash filling and clogging soil pore necks upon thin section analysis. In cases where the ash pore plugging effect does not occur, the ash layer may still limit the rate of infiltration into the two-layer soil system due to variation in hydraulic conductivity. For example, if ash hydraulic conductivity (K_{ash}) is less than soil hydraulic conductivity (K_{soil}) then the ash layer will dictate the infiltration rate (Moody *et al.* 2009; Kinner and Moody 2010). However, if $K_{ash} > K_{soil}$, the soil will regulate the rate of infiltration into the system, resulting in water ponding at the ash–soil interface (Onda *et al.* 2008; Woods and Balfour 2010). This response may promote saturation overland flow or subsurface storm flow, contributing to the initiation of debris flows (Cannon *et al.* 2001; Gabet and Sternberg 2008; Onda *et al.* 2008), but the overall runoff response of the system is also dependent upon rainfall rates and soil water storage capabilities. In cases where $K_{ash} > K_{soil}$, the ash layer also acts as a barrier, storing water rather than controlling infiltration (Kinner and Moody 2010; Woods and Balfour 2010). However, the ability of the ash layer to act as a barrier appears to be linked to ash moisture, as it has only been observed to occur under dry ash conditions (Moody *et al.* 2009; Kinner and Moody 2010).

Although research conducted by Onda *et al.* (2008) highlights that the mechanisms of runoff generation at the soil surface will change over time, the current study provides detailed observations that ash layer properties can change over time and thus the mechanisms of runoff generation could depend on these ash layer changes. This study provides direct documentation of ash crusting in the field and indicates that ash containing oxides and carbonates can crust and compact above the soil surface, reducing K_{ash}. This reduction in K_{ash} may contribute to the production of Hortonian overland flow depending upon the hydraulic conductivity of the underlying soil and changes in runoff mechanisms as outlined by Onda *et al.* (2008).

Implications for post-fire mitigation treatments

Robichaud *et al.* (2007) indicated that the presence of ash on the soil surface can be used as an indicator of soil burn severity and linked to increases in runoff and erosion, and therefore variation in ash has important implications for post-fire management. The documentation of ash crust formation presented in this study

supports the notion outlined by Cerdà and Doerr (2008) that burnt landscapes are the most susceptible to runoff and erosion following wind or rain events sufficient to remove the protective ash layer, but before the onset of vegetation recovery. Although the hydraulic conductivity of WR ash layers decreased by 1 order of magnitude with the formation of an ash crust, the conductivity was still higher (1×10^{-2} mm s^{-1}) than that of the underlying soil (1×10^{-3} mm s^{-1}), suggesting that the ash layer would not be the limiting infiltration layer within the soil system but instead continue to act as a capillary layer storing water (Kinner and Moody 2010; Woods and Balfour 2010). Although the low hydraulic conductivity of the underlying silt loam soil was consistent with other measurements of silt loams in the region (0.0025 mm s^{-1}; Woods and Balfour 2010), they are extremely small values, suggesting ash layers could act as the limiting infiltration layer atop more conductive soil types.

Results from this research also indicate that ash crust formation acted as a protective seal, reducing the removal of the ash layer: ash cover remained at 100% for 30 days in crusted plots and began to be removed via aeolian erosion after only 10 days in plots without crust formation (Fig. 7*a*). Visual observations of erosion associated with the larger rainfall event on 17 October in the WR area indicated that ash crust rilling occurred. However, the crust was still intact in places, suggesting that the stabilised ash layer may have protected the underlying soil from direct sheet-wash and inter-rill erosion (Fig. 5).

Ash is currently viewed as a valuable soil protectant against erosional agents, based on studies in Spain, Portugal and Lithuania (Cerdà and Doerr 2008; Zavala *et al.* 2009; Pereira and Úbeda 2010; Pereira *et al.* 2013), and the formation of an ash crust has the potential to decrease post-fire sediment yields by protecting the underlying soil from raindrop impact and soil sealing, similar to the effects of mulching. Further, depending upon ash depth, composition and plant species, the germination of post-fire vegetation may be aided by the long-term fertilisation associated with ash layers (Raison *et al.* 2009; Bodí *et al.* 2014). Overall, the noted response of a stabilised ash crust in a burnt watershed during this study suggests that ash layers could potentially be considered as a natural aid in reducing wind erosion as well as aiding in vegetation recovery: although it is very transient and further study is needed to assess these effects. Although precipitation and its temporal and spatial variability are often the primary drivers of post-wildfire runoff and erosion (Moody *et al.* 2013), it is important to make note of ash evolution and crusting. Ash layers have the ability to increase the rainfall threshold of the hillslope, as runoff generation occurs when the conductivity or storage capacity of the ash layer, which is proportional to thickness, is exceeded (Kinner and Moody 2010; Woods and Balfour 2010). Therefore, in order to fully assess the need for mitigation treatments after severe wildfires the ash layer should be taken into consideration.

Conclusions

This research was motivated by the need to understand how and to what extent ash layers change over time and if that temporal evolution could alter the hydrological response of post-fire ash layers. Although numerous authors have commented on the presence of an ash crust in post-fire ecosystem, the results from this study are the first to document the formation of an *in situ* ash crust after recent wildfire activity. Results indicate the following key findings:

(1) The formation of an ash crust can decrease ash hydraulic conductivity by 1 order of magnitude as well as significantly decreasing ash layer porosity and increasing bulk density.
(2) Although raindrop impact increased the robustness of an ash crust, raindrop impact alone is not sufficient to form an ash crust, rather mineralogical transformations must occur to produce a hydrologically relevant ash crust.
(3) Ash crust formation does not occur following all severe wildfire events. Initial ash composition, the presence of oxides and a hydrating rainfall event are all necessary precursors for crust formation.
(4) The formation of an ash crust can aid in stabilising the ash layer, potentially reducing aeolian mixing and erosion.

Acknowledgements

This manuscript is dedicated to the late Dr Scott W. Woods, whose contribution to Dr Balfour's research was paramount. He was a great mentor, scientist, teacher and friend, who will be missed by many, but forgotten by none. The authors thank Daniel Hatley, Jim Reilly, Keenan Storrar, Katie Jorgensen, Ian Hype and Lance Glasgow for aid in field data collection. This research was funded by grants from the National Science Foundation (Award# 1014938) and the US Department of Agriculture, Forest Service, Rocky Mountain Research Station (FSAN# 09-CS-11221634–283).

References

Balfour VN (2014) Determining wildfire ash saturated hydraulic conductivity and sorptivity with laboratory and field Methods. *Catena,* in press. [Published online early 11 February 2014]. doi:10.1016/J.CATENA.2014.01.009

Balfour VN, Woods SW (2013) The hydrological properties and the effects of hydration on vegetative ash from the Northern Rockies, USA. *Catena* **111**, 9–24. doi:10.1016/J.CATENA.2013.06.014

Bodí MB (2012) Ash and water repellency effects on soil hydrology in fire-affected Mediterranean ecosystems. PhD thesis, University of Valencia, Spain.

Bodí MB, Mataix-Solera J, Doerr SH, Cerdà A (2011) The wettability of ash from burned vegetation and its relationship to Mediterranean plant species type, burn severity and total organic carbon content. *Geoderma* **160**, 599–607. doi:10.1016/J.GEODERMA.2010.11.009

Bodí MB, Doerr SH, Cerdà A, Mataix-Solera J (2012) Hydrological effects of a layer of vegetation ash on underlying wettable and water repellent soil. *Geoderma* **191**, 14–23. doi:10.1016/J.GEODERMA.2012.01.006

Bodí MB, Martin D, Balfour VN, Santín C, Doerr SH, Pereira P, Cerdà A, Mataix-Solera J (2014) Wildland fire ash: production, composition and eco-hydro-geomorphic effects. *Earth-Science Reviews* **130**, 103–127. doi:10.1016/J.EARSCIREV.2013.12.007

Cannon SH, Kirkham RM, Parise M (2001) Wildfire related debris-flow initiation processes, Storm King Mountain, Colorado. *Geomorphology* **39**, 171–188. doi:10.1016/S0169-555X(00)00108-2

Cerdà A (1998) Changes in overland flow and infiltration after a rangeland fire in a Mediterranean scrubland. *Hydrological Processes* **12**, 1031–1042. doi:10.1002/(SICI)1099-1085(19980615)12:7<1031::AID-HYP636>3.0.CO;2-V

Cerdà A, Doerr SH (2008) The effect of ash and needle cover on surface runoff and erosion in the immediate post-fire period. *Catena* **74**, 256–263. doi:10.1016/J.CATENA.2008.03.010

Clothier B, Scotter D (2002) Unsaturated water transmission parameters obtained from infiltration. In 'Methods of Soil Analysis, Part 4: Physical

Methods'. (Eds JH Dane, GC Topp) pp. 879–896. (Soil Science Society of America: Madison, WI)
Dane JH, Hopmans JW (2002) Hanging water column. In 'Methods of Soil Analysis, Part 4: Physical Methods'. (Eds JH Dane, GC Topp) pp. 680–684. (Soil Science Society of America: Madison, WI)
DeBano LF, Neary DG Ffolliot PF (1998) 'Fire Effects on Ecosystems.' (Wiley: New York)
Decagon Devices (2006) Mini disk infiltrometer user's manual. (Decagon Devices: Pullman, WA) Available at http://www.decagon.com/products/hydrology/hydraulic-conductivity/mini-disk-portable-tension-infiltrometer/ [Verified 12 May 2014]
Ebel BA, Moody JA, Martin DA (2012) Hydrologic conditions controlling runoff generation immediately after wildfire. *Water Resources Research* **48**, W03529. doi:10.1029/2011WR011470
Etiégni L, Campbell AG (1991) Physical and chemical characteristics of wood ash. *Bioresource Technology* **37**, 173–178. doi:10.1016/0960-8524(91)90207-Z
Flint A, Flint L (2002) Particle density. In 'Methods of Soil Analysis, Part 4: Physical Methods', (Eds JH Dane, GC Topp) pp. 241–253. (Soil Science Society of America: Madison, WI)
Gabet EJ, Sternberg P (2008) The effects of vegetative ash on infiltration capacity, sediment transport and the generation of progressively bulked debris flows. *Geomorphology* **101**, 666–673. doi:10.1016/J.GEOMORPH.2008.03.005
Grossman RB, Reinsch TG (2002). Bulk density and linear extensibility. In 'Methods of Soil Analysis, Part 4: Physical Methods'. (Eds JH Dane, GC Topp) pp. 201–228. (Soil Science Society of America: Madison, WI)
Kinner DA, Moody JA (2010) Spatial variability of steady-state infiltration into a two-layer soil system on burned hillslopes. *Journal of Hydrology* **381**, 322–332. doi:10.1016/J.JHYDROL.2009.12.004
Larsen IJ, MacDonald LH, Brown E, Rough D, Welsh MJ, Pietraszek JH, Libohova Z, Benavides-Solorio JD, Schaffrath K (2009) Causes of post-fire runoff and erosion: water repellency, cover, or soil sealing? *Soil Science Society of America Journal* **73**, 1393–1407. doi:10.2136/SSSAJ2007.0432
Liodakis S, Katsigiannis G, Kakali G (2005) Ash properties of some dominant Greek forest species *Thermochimica Acta* **437**, 158–167. doi:10.1016/J.TCA.2005.06.041
Moody JA, Kinner DA, Ubeda X (2009) Linking hydraulic properties of fire affected soils to infiltration and water repellency. *Journal of Hydrology* **379**, 291–303. doi:10.1016/J.JHYDROL.2009.10.015
Moody JA, Shakesby RA, Robichaud PR, Cannon SH, Martin DA (2013) Current issues related to post-wildfire runoff and erosion processes. *Earth-Science Reviews* **122**, 10–37. doi:10.1016/J.EARSCIREV.2013.03.004
Munsell AH (1975) 'Soil Color Chart Handbook.' (USDA: Baltimore, MD)
Neary DG, Ryan KC, DeBano LF (2005) Wildland fire in ecosystems: effects of fire on soil and water. USDA Forest Service, Rocky Mountain Research Station, General Technical Report RMRS-GTR-42-Volume 4. (Ogden, UT)
Novara A, Gristina L, Bodí MB, Cerdà A (2011) The impact of fire on redistribution of soil organic matter on a Mediterranean hillslope under maquia vegetation type. *Land Degradation and Development* **22**, 530–536. doi:10.1002/LDR.1027
Onda Y, Dietrich WE, Booker F (2008) Evolution of overland flow after a severe forest fire, Point Reyes, California. *Catena* **72**, 13–20. doi:10.1016/J.CATENA.2007.02.003
Parsons A, Robichaud PR, Lewis SA, Napper C, Clark JT (2010) Field guide for mapping post-fire soil burn severity. USDA Forest Service, Rocky Mountain Research Station, General Technical Report RMRS-GTR-243. (Fort Collins, CO)
Pereira P, Cerdà A, Úbeda X, Mataix-Solera J, Martin D, Jordán A, Burguet M (2013) Spatial models for monitoring the spatio–temporal evolution of ashes after fire – a case study of a burnt grassland in Lithuania. *Solid Earth* **4**, 153–165. doi:10.5194/SE-4-153-2013
Pierson FB, Robichaud PR, Spaeth KE (2001) Spatial and temporal effects of wildfire on the hydrology of a steep rangeland watershed. *Hydrological Processes* **15**, 2905–2916. doi:10.1002/HYP.381
Raison RJ, Khanna PK, Jacobsen K, Romanya J, Serrasolses I (2009) Effect of fire on forest nutrient cycles. In 'Fire Effects on Soil and Restoration Strategies'. (Eds A Cerdà, PR Robichaud) pp. 225–256. (Science Publishers: Enfield, NH)
Robichaud PR (2000) Fire effects on infiltration rate after a prescribed fire in Northern Rocky Mountain forests, USA. *Journal of Hydrology* **231–232**, 220–229. doi:10.1016/S0022-1694(00)00196-7
Robichaud PR, Lewis SA, Laes DYM, Hudak AT, Kokaly RF, Zamudio JA (2007) Postfire soil burn severity mapping with hyperspectral image unmixing. *Remote Sensing of Environment* **108**, 467–480. doi:10.1016/J.RSE.2006.11.027
Robichaud PR, Lewis SA, Ashmun LE (2008) New procedure for sampling infiltration to assess post-fire soil water repellency. USDA Forest Service, Rocky Mountain Research Station, Research Note RMRS-RN-33. (Fort Collins, CO)
Santín C, Doerr SH, Shakesby RA, Bryant R, Sheridan GJ, Lane PNJ, Smith HG, Bell TL (2012) Carbon loads, forms and sequestration potential within ash deposits produced by wildfire: new insights from the 2009 'Black Saturday' fires, Australia. *European Journal of Forest Research* **131**, 1245–1253. doi:10.1007/S10342-012-0595-8
Schmidt MWI, Noack AG (2000) Black carbon in soils and sediments: analysis, distribution, implications and current challenges. *Global Biogeochemical Cycles* **14**, 777–793. doi:10.1029/1999GB001208
Schumacher BA (2002) Methods for the determination of total organic carbon (TOC) in soils and sediments. Environmental Protection Agency, Exposure Research Laboratory NCEA-C-1282. (Las Vegas, NV)
Stoof CR, Wesseling JG, Ritsema CJ (2010) Effects of fire and ash on soil retention. *Geoderma* **159**(3–4), 276–285. doi:10.1016/J.GEODERMA.2010.08.002
Úbeda X, Pereira P, Outeiro L, Martin DA (2009) Effects of fire temperature on the physical and chemical characteristics of the ash from two plots of cork oak (*Quercus suber*). *Land Degradation and Development* **20**, 589–608. doi:10.1002/LDR.930
Vandervaere J, Vauclin M, Elrick DE (2000) Transient flow from tension infiltrometers: II. Four methods to determine sorptivity and conductivity. *Soil Science Society of America Journal* **64**, 1272–1284. doi:10.2136/SSSAJ2000.6441272X
Wagenbrenner N, Lamb B, Robichaud PR, Germino G (2011) Measurement of PM_{10} emissions in a post-wildfire environment. In '3rd International Meeting of Fire Effects on Soil Properties', 15–19 March 2011, Guimarães, Portugal (Eds A Bento Gonçalves, A Vieira) pp. 64–68. (Universidade do Minho, Núcleo de Investigação em Geografia e Planeamento and CEGOT: Guimarães)
Woods SW, Balfour VN (2008) Effect of ash on runoff and erosion after a severe forest wildfire. Montana, USA. *International Journal of Wildland Fire* **17**, 535–548. doi:10.1071/WF07040
Woods SW, Balfour VN (2010) Variability in the effect of ash on post-fire infiltration due to differences in soil type and ash thickness. *Journal of Hydrology* **393**(3–4), 274–286. doi:10.1016/J.JHYDROL.2010.08.025
Zavala LM, Jordán A, Gil J, Bellinfante N, Pain C (2009) Intact ash and charred litter reduces susceptibility to rain splash erosion post-wildfire. *Earth Surface Processes and Landforms* **34**, 1522–1532. doi:10.1002/ESP.1837